Long-Period Tidal Forcing of Indian Monsoon Rainfall: An Hypothesis

WILLIAM H. CAMPBELL, JEROME B. BLECHMAN[1] AND REID A. BRYSON

Center for Climatic Research, Institute for Environmental Studies, University of Wisconsin-Madison

(Manuscript received 5 May 1982, in final form 5 November 1982)

ABSTRACT

This paper examines the nature of the periodic components observed in the interannual variability of June rainfall in northern India by using an eigenvector analysis of the spectra of the June rainfall record (1895–1975) and an eigenvector analysis of the precipitation data itself for stations in that region. The first eigenvectors of these analyses have similar spatial and spectral characteristics which indicate that in June the atmosphere in northern India responds strongly at two frequencies, 0.05 and 0.26 year^{-1}. These two frequencies match the two dominant frequencies in the spectrum of a time series (1895–1975) of the mean monthly soli-lunar tidal potential at the latitude of northern India. It is hypothesized that tidal effects modulate the advance of the monsoon "front", producing some of the observed interannual variability. This hypothesis has been tested by using the tidal frequencies to predict June rainfall a year in advance. The success rate of these year-in-advance forecasts in northern India, on independent data, significantly exceeded that expected by chance or predicted by interannual persistence, suggesting that mechanical tidal forcing might be a useful additional long-range forecast tool.

1. Introduction

Interannual variability of climate may be viewed as consisting of at least two components: a nonlinear secular component and a complex periodic component. There may be a random third component, but since that component may be simply that part of the variability which is as yet unexplained we will not consider it further here. We assume instead that all climatic variations are deterministic unless proven otherwise. Our purpose is to identify those portions of the variability which are predictable and might contribute to usable, even if imperfect, long lead-time forecasts of temperature or precipitation. By long lead-time we mean one or more years in advance.

In this paper we examine whether there are important periodic components observed in the interannual variability of June rainfall in India. Two periodicities in fact do dominate the spectra of June rainfall records for stations in northern India. The question to be answered is what can produce a periodic response in June rainfall amounts. One possibility is a thermal forcing. Bryson and Goodman (1980) have shown that the variations in the amount of solar radiation reaching the ground have significant periodic components, but not at sunspot frequencies. Another possibility is the periodic, mechanical forcing produced by the "pole tide" associated with the Chandler wobble (Bryson and Starr, 1977) or by the long-period gravitational tides associated with the earth-sun-moon interaction (i.e., soli-lunar tides).

The last causal mechanism mentioned above is of particular interest. The moon's gravitational force has been considered for many years as a possible source of periodicities observed in weather data (Adderley and Bowen, 1962; Brier and Bradley, 1964; Mills, 1966; Lund, 1965). Characteristically, each of these authors describes the variability of a particular parameter such as rainfall at individual frequencies also exhibited in lunar tides. Few, if any, of these ideas find their way into practical use, mainly because the arguments are usually statistical and linear and because the forces involved are generally felt to contribute trivially to the total atmospheric response. We shall consider a case where soli-lunar tidal forcing apparently contributes in a significant manner to that part of the rainfall variance which lies in the interannual range.

The diurnal and semi-diurnal tides in the ocean and atmosphere are well-known manifestations of the lunar tides. However, as shown by Bryson (1948) and discussed by Brier (1968), the longer period lunar tides may be more important in the atmosphere in that they may cause shifts in the geographic locations of steady or regular features, such as subtropical anticyclones. Such shifts would result in large departures from normal in the areas where the gradients are the largest.

In order to study soli-lunar tides and their effect on the monthly characteristics of the climate at the interannual scale, it was necessary to generate time series of the *monthly mean* soli-lunar tidal potential which has been described quantitatively by Doodson (1921). A time series of the monthly mean horizontal soli-lunar force can then be calculated by taking the negative gradient of this potential. This results in X

[1] Present affiliation: Earth Science Department, State University College, Oneonta, NY 13820.

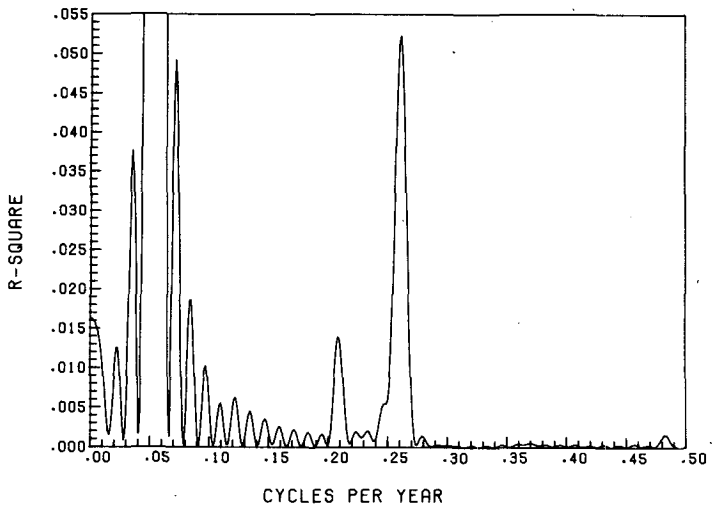

FIG. 1. A periodogram of the mean monthly soli-lunar tidal potential for the month of June at 25°N, 75°E for the period 1895 through 1975. The peak at 0.054 year^{-1} has a value of 0.928.

and Y components of the force. Time series of the soli-lunar tidal potential and of the X and Y components of the force were developed for a location in northern India (25°N, 75°E) and for another location in southern India (10°N, 78°E) for the period 1895–1975 which coincided with the available monthly precipitation data.

Periodograms of each of these two June monthly-mean tidal potential time series had their two largest peaks at 0.054 year^{-1} and at 0.262 year^{-1}, indicating that long-period soli-lunar tides act predominantly at these frequencies in the tropics. The periodogram for the tidal potential at 25°N, 75°E is shown in Fig. 1. The resolution of this periodogram is 0.1 cycles per 81 years (0.0012 year^{-1}), so the frequencies at the peaks are quite accurately specified. With these frequencies in mind we set out to see if we could find them in the June precipitation data.

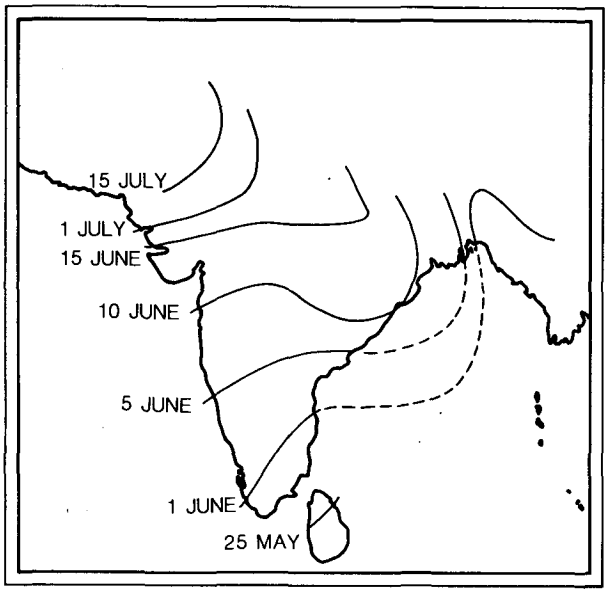

FIG. 2. The normal dates of the onset of the monsoon (figure adapted from Das, 1968, see text).

We will first describe the nature of the interannual variability of June rainfall in northern India and then put forth a working hypothesis that appears to explain and be quite consistent with the observations. We will then provide results of climatic predictions based on this hypothesis, for in addition to explaining the past behavior of the climate, a valid hypothesis of this type should also be able to predict the future climate.

It should be emphasized that in this paper we are dealing with interannual variability of June precipitation, which in northern India is about 38% of the intra-annual variance of monthly precipitation and, thus, equals only 1–2% of the daily variance (if one considers that the variance of monthly precipitation amounts is about 1/30 that of the daily variance). Therefore, even if soli-lunar tides account for a very small fraction of the total variance, this forcing becomes a candidate causal factor to consider when trying to understand *interannual* variability.

The frequency distribution of rainfall amounts for a given month can be highly skewed especially in the drier regions of India. If the data are not normally distributed, standard regression significance tests do not apply. To reduce the skewness, the precipitation data were subjected to a cube-root transform. This makes the frequency distribution at a given station

more nearly normal. The cube-root transform did not change the frequency structure of the precipitation spectra.

2. Characteristics of interannual variability of June rainfall in India

June is the month of the monsoon onset over most of the Indian subcontinent. The onset can be viewed as a front (Das, 1968) which, on the average, enters the southeastern tip of India around 1 June and ends up near the Pakistani–Indian border by 1 July (Fig. 2). Prior to monsoon onset, India is basically dry and hot except for scattered pre-monsoon showers. When the monsoon front arrives there is a tremendous burst of precipitation. However, once the monsoon front is past, the cloud tops are generally not very high and drizzle to light rain is the predominant form of precipitation with intervals of heavier rainfall and deeper convection associated with monsoon depressions from the Bay of Bengal.

There is considerable variability in the date of onset from year to year. For example, along the west coast south of 20°N the standard deviation of the onset is about seven days (Rao, 1976). It is the variability in onset date which greatly affects the June precipitation pattern in northern India, where the advance of the monsoon front begins to slow down. In this region small displacements of the monsoon front with its associated large rainfall gradient will markedly affect the amount of rainfall received in June. If the monsoon front is late, a significant percentage of the opportunity for rain in the calendar month of June is lost, because the pre-monsoon days are drier than the normal post-monsoon "burst" days. Thus, small anomalies in the monsoon front's normal position can be seen in the year-to-year fluctuations of June rainfall amounts at stations in northern India. For example, if the normal date of arrival of the monsoon is 25 June, a two-day delay in arrival time represents a 40% reduction in the duration of June monsoon rains. By contrast, at stations in southern India, where the monsoon normally arrives in May or early June, a two-day delay in arrival of the rains would have a small percentage effect on June rainfall. Furthermore, in northern India the monsoon front moves slowly, on the order of 25–50 km day^{-1}, so that quite small spatial departures from the normal position represent significant advances or delays in arrival time.

An eigenvector analysis of the spectra of June rainfall at 46 stations located throughout India for the period 1895–1975 provides insight into the nature of the interannual variability. In this analysis the variables are the frequency bands of the spectra which were calculated by using a Fast Fourier Transform (FFT). The observations are the percent variance for a given frequency at each of the stations. Thus, with

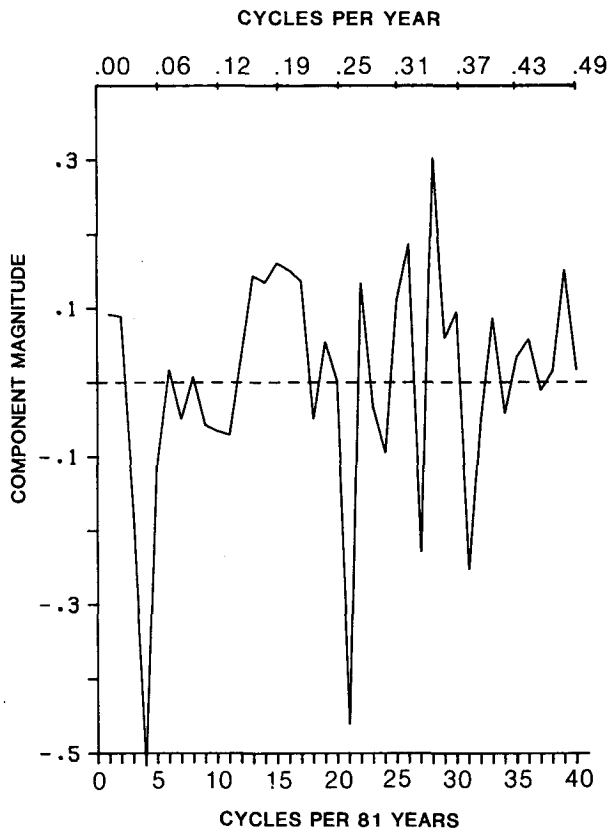

FIG. 3. The first eigenvector of the spectra of precipitation records at 46 stations on the Indian subcontinent for the period 1895–1975. The numbers plotted are the magnitudes of the components of this eigenvector. This eigenvector accounts for 13.5% of the interstation variance.

81 years of data there are 40 bands, or variables, and since there are 46 stations being considered, there are 46 observations for each band. The eigenvectors themselves are the orthogonal components of a given station's spectrum. When the eigenvectors are weighted by their coefficients at a given station and then added together, the result is the spectrum for that station. A plot of the coefficients produces a map showing which areas of India are dominated by a particular eigenvector and hence which frequencies are important in that area.

For example, the most striking feature of the first eigenvector from the analysis described above (shown in Fig. 3) is the presence of two large, negative peaks of this component of the spectrum at bands 4 and 21 (0.05 and 0.26 year^{-1}, respectively). Thus, stations dominated by eigenvector 1 with a negative coefficient would have a spectrum of June precipitation with a lot of power in these two bands. A map of the coefficients for this eigenvector (Fig. 4) shows a very coherent spatial pattern and indicates that the region most strongly dominated by negative coefficients of

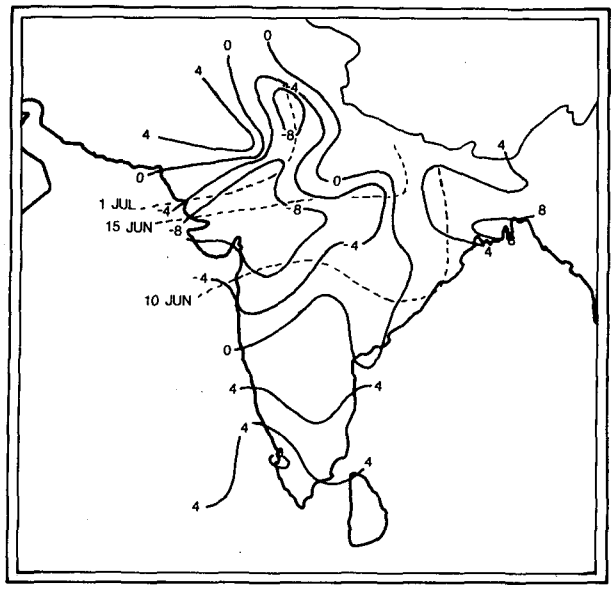

FIG. 4. The coefficients of the first eigenvector in Fig. 3. The coefficients have been multiplied by a factor of 100 before plotting. Three normal monsoon onset "frontal" positions from Fig. 2 are superimposed (dashed lines).

this eigenvector lies between the 10 June and 1 July average positions of the monsoon front.

Stations dominated by eigenvector 1 with large positive coefficients would have spectra characterized by a peak at 0.35 year^{-1} with little power at 0.05 or 0.26 year^{-1}, while stations dominated by eigenvector 1 with negative coefficients would have spectra characterized by power at both 0.05 and 0.26 year^{-1}. Thus, an eigenvector analysis of the spectra enables one to identify which frequencies are dominant for the area of study; and, in addition, the sign of the eigenvector component indicates which of these main frequencies appear together in a certain region and which are mutually exclusive.

The first eigenvector from the analysis described above (shown in Fig. 3) accounts for 13.54% of the variance. Here the variance refers to interstation variance since the observations consist of values from each station for a given frequency. In order to determine the significance of this eigenvector, 100 randomization experiments were run in a manner similar to the Monte Carlo technique described by Overland and Preisendorfer (1982). Each test consisted of generating 46 random 81-year time series, cube-rooting the data, normalizing the time series, calculating the 46 FFTs, and then performing an eigenvector analysis on these 46 spectra. Following the work of Overland and Preisendorfer (1982), after ordering the fractional explained variance for the first eigenvector of each of the 100 tests, the resulting distribution is represented by the 5th and the 95th values as [0.0812, 0.1042]. Since the fractional variance accounted for in our analysis (i.e., 0.1354) exceeds the 95th value, using their rule N, we can conclude that this eigenvector can in fact be distinguished from a random process. The value 0.1354 also exceeded the 100th value of the random test distribution. Thus there is less than a 1 in 100 chance that the first eigenvector in this analysis resulted from a random process. This distribution of fractional explained variance for the 100 random experiments is approximately normal (as determined by the Kolmogorov-Smirnov and chi-square goodness-of-fit tests with rejection criteria set at the 95% level). The mean and standard deviation of this distribution are 0.09233 and 0.00813, respectively. Thus, the value 0.1354 is 5.30 standard deviations away from the mean for a chance occurrence. Since the cumulative probability of a normal distribution at 5.3 standard deviations is 0.999999940, it is highly improbable that eigenvector 1 results from a random process.

The first eigenvector of the normalized precipitation data for the 46 station data set is shown in Fig. 5. The region dominated by this eigenvector also lies between the 10 June and 1 July monsoon front positions. The time series of the coefficients of this eigenvector is shown in Fig. 6a. A periodogram of this coefficient time series (Fig. 6b) produces two peaks—one around 0.05 year^{-1} and the other around 0.26 year^{-1}. This eigenvector, which is one of 46, accounts for 20.3% of the June rainfall variance.

Using Table 1 from Overland and Preisendorfer (1982), a conservative significance test for this eigenvector analysis with a data set of 46 variables and 81

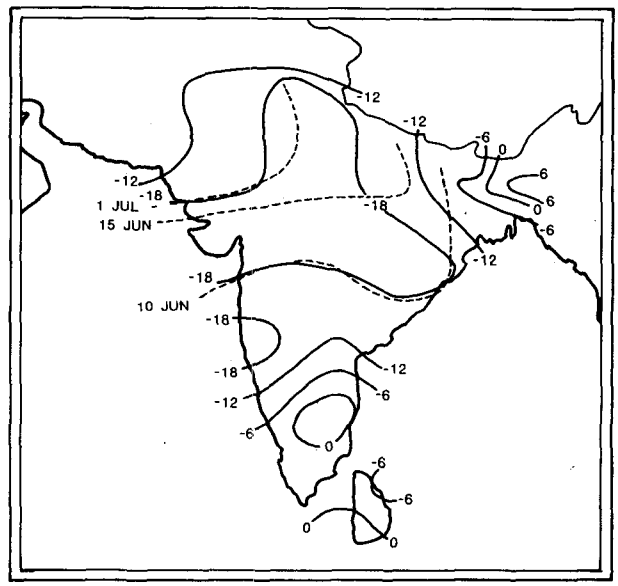

FIG. 5. The first eigenvector of the precipitation data for the 46 station data set (1895–1975). The values have been multiplied by a factor of 100 before plotting. This eigenvector accounts for 20.3% of the June rainfall variance. Monsoon frontal positions are superimposed as in Fig. 4.

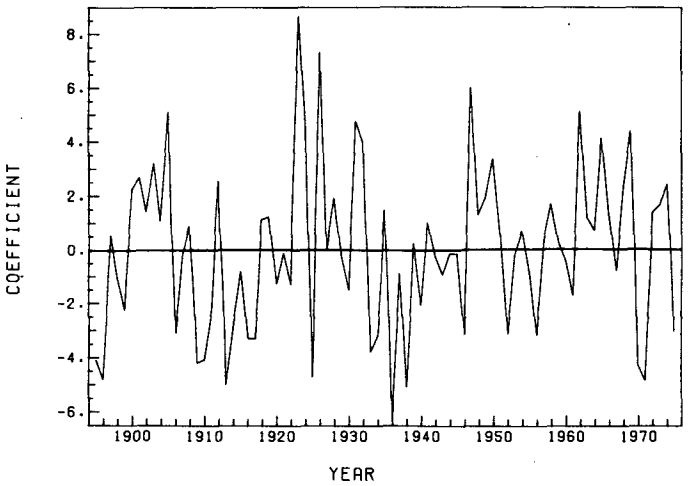

FIG. 6a. The time series plot of the coefficients for the first eigenvector of June precipitation shown in Fig. 5.

observations would be to use the value for 36 variables and 60 observations. To be significant, at the 95% level, the first normalized eigenvalue must explain 8.69% of the variance. Since eigenvector 1 in our analysis explained 20.3% of the variance, it represents a significant signal that can be distinguished from noise. The two peaks of the periodogram in Fig. 6b near 0.05 and .26 year^{-1} account for 17.2 and 15.1% of the variance, respectively. Since the periodogram of the eigenvector coefficients was calculated for each tenth of a frequency band individually, a standard F test with two predictors and 81 observations (78 degrees of freedom) yields confidence levels for the two peaks of 0.999 and 0.998, respectively.

The first eigenvector explains the greatest amount of variance, and its interpretation often leads to greater understanding of the physics governing the climatic situation. Comparison of Figs. 4 and 5 indicates that the spatial patterns of both the eigenvectors of the precipitation spectra and the precipitation data align themselves quite well with the positions of the monsoon front during the last part of June when the monsoon is advancing more slowly. Both eigenvectors are also associated with the same two dominant frequencies. The fact that the first eigenvector of the precipitation spectra and the first eigenvector of precipitation itself each yield similar spatial and spectral characteristics indicates that in June the atmosphere in northern India responds strongly at the two frequencies of 0.05 and 0.26 year^{-1}. Thus, any hypothesis that attempts to explain the interannual variability of June rainfall amounts in northern India

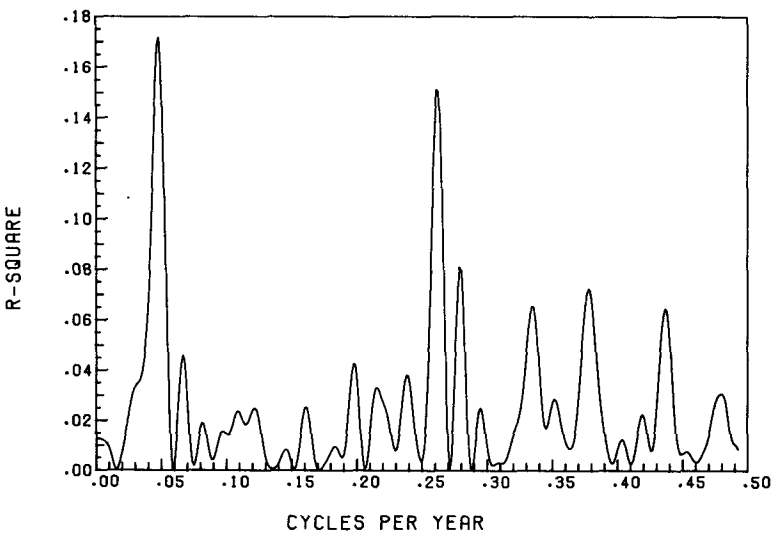

FIG. 6b. A periodogram of the coefficients of the first eigenvector of precipitation.

must be able to account for these *two* dominant frequencies.

3. A working hypothesis

One might develop an hypothesis based on the sunspot cycle because of the spectral peak at nearly 0.05 year^{-1}, but such an approach does not account for the second peak at 0.26 year^{-1}. Other hypotheses might also be put forth. We have developed a working hypothesis based on soli-lunar tidal forcing of the atmosphere because it is a geophysical mechanism that can account for both spectral peaks. Simply stated the hypothesis is that mechanical soli-lunar tidal effects on the atmosphere modulate the monsoon frontal position, resulting in *an element* of the interannual variability of June rainfall observed in northern India. As discussed earlier, this is the region where small anomalies in the monsoon frontal position can have a significant effect on the amount of rain received in June.

The two peaks observed in the soli-lunar tidal potential periodograms (Fig. 1) result from characteristics of the moon's orbit. One characteristic (and there are others) which contributes to the peak around 0.26 year^{-1} is the lunar synodic period. The mean lunar synodic period, 29.5306 days, is the time from new moon to new moon and represents the period of revolution of the moon around the earth with respect to the sun (Smart, 1971). There are two tidal maxima per synodic period. One-half of the synodic period would have 24.7365 cycles in a mean solar year. This frequency aliases at about 0.26 year^{-1} when sampling is done once per calendar year. The calculated soli-lunar tidal potential is the net effect of all earth-sun-moon tidal interactions combined and is completely deterministic, but it is time-dependent because the moon's orbit around the earth is perturbed by the sun's gravitational attraction which varies with the earth-sun distance. As a result, the frequency is a function of the exact time interval over which it is calculated. Thus, the 0.262 year^{-1} frequency calculated for the 1895–1975 period, as seen in Fig. 1, is the result of forcing at the half-synodical month period and at several other periods which also alias there. That this cycle is manifested in a periodogram of tidal potential sampled on a once per year basis is hardly surprising. However, it is noteworthy that the frequency is also found in meteorological data, as shown in the preceding section. The other lunar spectral peak at 0.054 year^{-1} is associated with the nodal period, which is the time it takes the pole of the moon's orbit to revolve once about the pole of the ecliptic. Currie (1981) provides interesting evidence of this frequency in North American temperature and drought data.

Comparison of the periodogram of the first eigenvector of June precipitation (Fig. 6b) with that of the horizontal soli-lunar tidal potential (Fig. 1) coupled with the eigenvector analysis of June precipitation spectra (Fig. 3) strongly suggests that the year-to-year fluctuations in the precipitation of northern India might result from tidal forcing. Furthermore, since the June rainfall amounts at northern Indian stations are dominated by the location of the station relative to the monsoon front during the month, it seems reasonable that modulation of the monsoon frontal position is the cause of the observed anomalies. It appears unlikely, however, that the modulation is due to a direct tidal forcing on the front itself. It may be that the soli-lunar forcing shifts the position of a "center of action" (e.g., the South Indian Ocean high) in a periodic fashion as Bryson (1948) showed for the eastern Pacific high. If so, this periodic movement may affect the delicate momentum balance which determines how the monsoon front advances and subsequently produces a response in the June rainfall data with a similar periodicity.

Another possible explanation may be that the soli-lunar forcing affects sea surface temperatures (SSTs) as Picaut and Verstraete (1979) have shown. They found periodicities around the lunar fortnightly and half-synodical periods in travelling waves along the northern coast of the Guinea Gulf. These waves affect the thermal structure of the ocean with the associated SST oscillation possibly reaching 2.5°C in the upwelling season. This in turn would influence the atmospheric temperature. Many authors have related equatorial Pacific SSTs (e.g., Bjerknes, 1969; Rasmusson and Carpenter, 1982) to the Southern Oscillation which exhibits periodicities in the 3–6 year range (which includes the 3.8-year period discussed in this paper). Since this phenomenon is correlated with Indian precipitation (Walker, 1924), it may be that the 0.26 year^{-1} frequency observed in Indian June precipitation is indirectly related to tidal forcing via the oceans and the ocean-atmosphere feedback characteristic of the Southern Oscillation. However, this relationship is not as good as one might hope, for the periodicities found in the Southern Oscillation index are not constant in time according to Wright (1978) and Rasmusson and Carpenter (1982). If the coefficients of the first eigenvector of June precipitation are split into two independent time series (1895–1935 and 1936–1975), there are peaks at 0.2634 year^{-1} (16.9% of the variance) and 0.265 year^{-1} (14.2% of the variance), respectively, indicating that this frequency is dominant throughout the 81 years of data. Further analysis is required to assess any connection between June precipitation in India and the Southern Oscillation.

Both the periodogram of the first eigenvector of June precipitation (Fig. 6b) and that of the horizontal soli-lunar tidal potential (Fig. 1) have peaks at 0.262 year^{-1}. Both also have peaks around 0.05 year^{-1}; how-

ever, the soli-lunar tidal potential peak is at 0.054 year^{-1} and the precipitation peak appears at 0.048 year^{-1}. We must account for this difference if we assume that it is the forcing acting at the nodal period and the half-synodic period that directly results in the observed precipitation response through the possible mechanisms suggested above. The difference may be due to the fact that in an 81-year time series a period of around 20 years cannot be very accurately defined. This may well be the case. However, another more appealing alternative is that the soli-lunar forcing responsible for the periodicities observed in the precipitation data results from an amplitude modulation of the lunar fortnightly tide (13.6061 days or 26.8440 year^{-1}) by forcing at the semi-nodal period (9.3067 years or 0.1074 year^{-1}). This modulation, given by

$$A\cos(X)\cos(Y) = A/2[\cos(X+Y) + \cos(X-Y)],$$

results in the two frequencies, 26.951 and 26.737 year^{-1} which would alias at .049 year^{-1} and at .263 year^{-1}. Mathematically, the amplitudes at these frequencies should be equal. These two hypothesized frequencies come very close to those observed in the precipitation data and the amplitudes of the observed frequencies are very similar as seen in Fig. 6b.

Further research is required to determine whether it is the two frequencies observed directly in the soli-lunar tidal potential or the two frequencies resulting from the nonlinear amplitude modulation described above (or neither) that result in the interannual variability observed in the precipitation data.

Physically the amplitude modulation hypothesis has a good basis. Bryson (1948), in a study which was later corroborated by Brier (1968), found convincing evidence of a lunar fortnightly tidal periodicity in the latitudinal position of the subtropical anticyclones. All that has been added here is an amplitude modulation of this periodicity. Movement of the subtropical highs is directly related to movement of the subtropical jet and the subtropical jet has been shown to be strongly connected to the onset of the Indian monsoon (Yin, 1949; Wright, 1967).

If one assumes that the two peaks of the first eigenvector of June precipitation (Fig. 6b) are the result of forcing at either the two dominant soli-lunar tidal frequencies of Fig. 1 or the two frequencies resulting from the amplitude modulation of the lunar fortnightly tide, then another question comes to mind: What is the probability that the two peaks of Fig. 6b might occur by chance at either of these two hypothesized sets of frequencies? To determine this probability another randomization test was performed. The data for the 46 stations were scrambled by year (but not by station or by stations within years). This preserves the spatial but not the temporal coherence. As a result, the correlation matrix is unchanged, resulting in identical eigenvector components but scrambled eigenvector coefficients. Therefore, to determine the empirical probability, 100 periodograms were produced from randomly ordered sequences of the 81 coefficients for eigenvector 1. In no case were the two highest peaks within ±0.01 cycle year^{-1} of the two soli-lunar tidal potential periodogram peaks (i.e., they were not between 0.044 and 0.064 year^{-1} or between 0.252 and 0.272 year^{-1}) nor were they within ±0.01 cycle year^{-1} of the other two-frequency set, 0.049 and 0.263 year^{-1}. Thus, the probability that two such peaks would occur by chance appears to be less than 1 in 100.

4. Forecasting test

Since tidal forces are predictable, we have used our hypothesis to make predictions of monthly rainfall and have verified those predictions. Forces contributing trivially to interannual variance cannot, in the long run, be expected to give forecasts which are better than those made by chance. Conversely, if soli-lunar tidal forces do cause nontrivial atmospheric responses and this interaction can be incorporated into a forecast method, predictions which can be shown to be better than chance might be expected.

To make the forecasts, we linearly regressed the two tidal potential frequencies against the precipitation data at a given station to obtain one year forecasts for each year of the period 1961–75. To retain a large number of degrees of freedom we used only these two frequencies.[2] The regression equation is

$$F(t) = A_1\cos(2f_1t + \phi_1) + A_2\cos(2f_2t + \phi_2), \quad (1)$$

where

$F(t)$	regression forecast of monthly rainfall
t	time in years
f_1	$= 0.0530$ year^{-1}; $f_2 = 0.2606$ year^{-1}
A_1, A_2	regressed amplitudes
ϕ_1, ϕ_2	regressed initial phase angles.

The data through 1960 were the dependent data set and the data from 1961–75 were the independent (or test) data set. The tidal frequencies used for the forecasting (0.0530 year^{-1} and 0.2606 year^{-1}) were taken from a periodogram similar to Fig. 1 except that it covered only the dependent data period (1895–1960). A forecast for 1961 is made by calculating the regression coefficients using data up through 1960; a forecast for 1962 is made by recalculating the coefficients using data up through 1961, etc. We then have up to 15 one-year forecasts for each station

[2] Note added in proof: It now appears that the two frequencies observed in the precipitation data can be obtained if the two postulated soli-lunar forcing frequencies are modulated by a long-term fluctuation arising from a source other than the orbital characteristics of the earth-moon-sun system.

TABLE 1a. Results of persistence and regression forecasts for 15 Indian stations located between the 10 June and 1 July mean positions of the monsoon onset front. Number correct refers to a two-category test on independent data after 1961 (above or below mean) and 2×2 refers to the skill score on this test. Explained variance in percent is denoted R^2. The significance of R^2 in percent denoted Sig(W) when compared to a white spectral background and Sig(A) when autocorrelation or "red noise" is taken into account.

Station			Persistence		Regression				
WMO	Name	Forecasts	Correct	2×2	Correct	2×2	R^2	Sig(W)	Sig(A)
42099	Ludhiana	13	7	0.077	10	0.538	24.0	99.9	99.9
42147	Mukteswar	14	6	−0.143	8	0.143	7.3	81.1	77.7
42182	New Delhi	15	6	−0.200	9	0.200	10.5	93.9	96.4
42261	Agra	14	8	0.143	7	0.000	12.5	97.1	98.1
42391	Darbhanga	13	5	−0.231	8	0.231	4.3	53.1	52.2
42451	Kota	13	6	−0.077	9	0.385	16.5	99.4	98.5
42475	Allahabad	15	6	−0.200	8	0.067	21.7	99.9	99.8
42587	Daltonganj	13	5	−0.231	6	−0.077	5.4	65.7	67.9
42647	Ahmadabad	15	11	0.467	9	0.200	9.8	92.1	88.2
42671	Sagar	15	10	0.333	10	0.333	15.0	98.9	97.2
42731	Dwarka	15	7	−0.067	11	0.467	9.8	92.1	92.3
42754	Indore	15	7	−0.067	10	0.333	19.0	99.8	99.8
42867	Nagpur	15	8	0.067	11	0.467	4.1	50.5	46.6
42909	Veraval	15	5	−0.333	8	0.067	8.1	85.6	86.5
42970	Cuttack	12	7	0.167	8	0.333	12.1	96.6	95.6
	Total	212	104	−0.019	132	0.245	—	—	—

which can be compared to what actually happened, and thus establish whether or not we have achieved forecasting skill beyond what would be expected by chance. The regressions for the 46 stations used in the eigenvector analysis are summarized in Table 1. These 46 stations were divided into two groups—the 15 stations which lie between the 10 June and 1 July average positions of the monsoon front (Table 1a) and the 31 stations which do not (Table 1b). One would expect good forecasts in the former region and poorer forecasts in the latter. Fig. 7 shows the location of the 46 stations with the two positions of the monsoon front delineating the 15 station subset.

One of the diagnostic quantities computed was the explained variance as a fraction of the total interannual variance. Only four parameters (A_1, A_2, ϕ_1, ϕ_2) were required to completely specify $F(t)$ in (1). For that small number of predictors, some of the explained variance values were quite high (see Table 1) especially in the region of the 15 station subset. F-tests were used to assess the significance of these values. Assuming a white spectrum, i.e., little autocorrelation, 7 of the 15 station subset, located between the 10 June and 1 July monsoon onset positions, passed at the 95% level where only 0–1 would be expected by chance. Assuming lag-1 autocorrelation (i.e., red spectra) did not alter these results substantially.

The verification results for these forecasts are given in Table 1 in terms of 2×2 skill scores. A forecast was considered correct if it had the same sign of departure from the record mean as the observed data. Random forecasts would be expected to score 50% on this basis, even with skewed rainfall distributions, since the cube-root normalization procedure corrects partially for skewness and the forecasts are distributed equally about the mean.

Out of the 212 forecasts made for the 15 stations in northern India 62.3% (132 forecasts) were correct. If it is appropriate to use the binomial distribution of discrete forecast events, the probability that these forecast results were not achieved by chance is 0.9999. While precipitation data generally possess little or no spatial coherence (Walsh and Mostek, 1980; Kidson, 1975), the 212 forecasts are probably not completely independent. The true number of independent forecasts is unknown. However, if the number is halved (66 correct out of 106), the probability of being nonrandom only drops to 0.9958 and if the number of forecasts is quartered (33 correct out of 53), the probability is still 0.9733. Considering the forecasts made for the other 31 stations, 54.8% of the 425 forecasts were correct. Persistence of anomalies from one year to the next was also evaluated as a control predictor. The results for the 15 station subset, for the other 31 stations, and for all 46 stations were less than 50% correct. Persistence forecasts tended to show negative skill. Forecasts were also made using the two-frequency model, 0.049 year^{-1} and 0.261 year^{-1}. The results were similar to those just described but the difference between the percent correct for the forecasts for the 15 and 31 station subsets was not as great.

Thus, the two soli-lunar frequencies provided year-in-advance forecasting skill precisely in the region where our hypothesis predicted their effect should be

TABLE 1b. As in Table 1a, but for 31 stations located outside the 10 June and 1 July mean positions of the monsoon onset front.

Station			Persistence		Regression				
WMO	Name	Forecasts	Correct	2 × 2	Correct	2 × 2	R^2	Sig(W)	Sig(A)
41530	Peshawar	15	6	−0.200	10	−0.333	9.0	89.2	92.0
41640	Lahore City	15	6	−0.200	10	0.333	17.9	99.7	99.7
41661	Quetta	15	11	0.467	9	0.200	6.6	76.3	70.4
41696	Kalat	13	6	−0.077	6	−0.077	2.2	22.8	27.1
41782	Karachi	15	7	−0.067	9	−0.200	12.4	97.0	98.2
42165	Bikaner	11	4	−0.273	7	0.273	2.2	22.8	25.0
42295	Darjeeling	11	6	0.091	6	0.091	12.4	97.0	95.5
42339	Jodhpur	15	9	0.200	11	0.467	13.8	98.3	98.3
42404	Dhubri	12	5	−0.167	3	−0.500	2.6	28.9	26.1
42411	Gauhati	15	7	−0.067	9	0.200	2.1	21.3	19.7
42515	Cherrapunji	10	3	−0.400	6	0.200	1.6	14.0	12.4
42599	Dumka	13	7	0.077	7	0.077	7.1	79.8	79.4
42619	Silchar	13	6	−0.077	7	0.077	3.5	42.3	39.9
42807	Calcutta	15	7	0.067	7	−0.067	3.7	45.1	43.9
42933	Akola	15	7	−0.067	9	0.200	9.9	92.3	89.9
43057	Bombay	15	7	−0.067	8	0.067	6.0	71.4	68.3
43063	Poona	15	9	0.200	9	0.200	12.5	97.1	96.5
43128	Begampet	13	8	0.231	9	0.385	2.7	30.4	28.5
43149	Vishakhapatnam	15	7	−0.067	7	−0.067	6.7	77.0	77.3
43185	Masulipatam	15	7	−0.067	7	−0.067	6.3	73.9	69.1
43197	Belgaum	14	7	0.000	10	0.429	18.8	99.8	99.8
43279	Madras	15	9	0.200	10	−0.333	3.0	34.9	28.1
43283	Mangalore	15	4	−0.467	8	−0.067	2.7	30.4	28.6
43295	Bangalore	15	6	−0.200	7	−0.067	4.3	53.1	55.5
43351	Fort Cochin	12	6	0.000	7	0.167	5.8	69.6	66.1
43363	Pamban	15	5	−0.333	4	−0.467	3.0	34.9	36.3
43369	Minicoy	14	6	−0.143	8	0.143	7.4	84.5	81.7
43371	Trivandrum	15	4	−0.467	6	−0.200	3.3	39.4	38.9
43418	Trincomalee	12	3	−0.500	6	0.000	6.6	76.3	74.7
43466	Colombo	12	7	0.167	5	−0.167	2.4	25.8	22.1
43540	Srinagar	10	5	0.000	6	0.200	8.4	87.0	88.4
	Total	425	197	−0.073	233	0.096	—	—	—

important. In addition, these forecasts appear to be significantly better than both persistence and chance.

5. Conclusions

We have shown that the monthly June rainfall totals in northern India have a very well defined spectral signature with two dominant modes of variation at around 0.05 and 0.26 year^{-1}. We have also shown that the spectral characteristics of the monthly mean soli-lunar tidal potential in northern India are similar to those seen in the rainfall data with spectral peaks near the lunar nodal cycle (0.054 year^{-1}) and near the aliased half-synodic month period (0.262 year^{-1}). The rainfall spectral peaks may also be the result of amplitude modulation of the lunar fortnightly tide at the semi-nodal period. In either case the hypothesis of soli-lunar forcing appears to be an attractive one.

An hypothesis that this tidal forcing modulates the position of the monsoon onset front in northern India, where the front moves more slowly than in the south, has been proposed. This modulation apparently delays or advances the beginning of monsoon rains enough to cause large June rainfall anomalies.

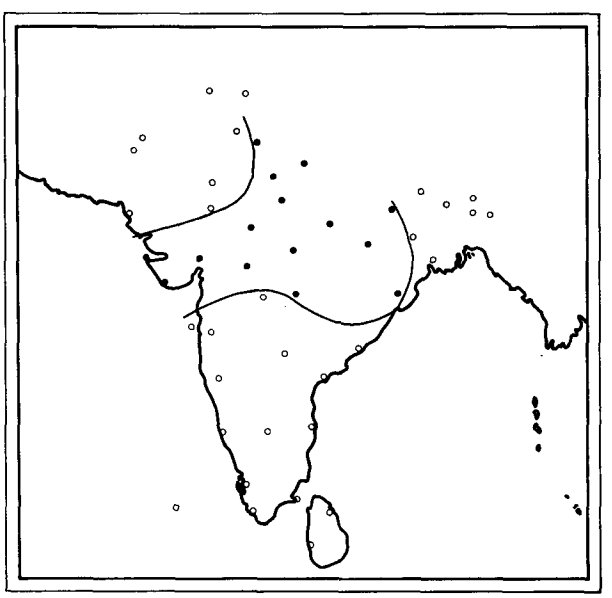

FIG. 7. Locations of the 46 stations used for the eigenvector analyses and for the forecasts. The blackened circles identify the 15 station subset located between the 10 June and 1 July average position of the monsoon front.

At present we can only speculate on the mechanism by which the tidal forces modulate the monsoon front position.

One year forecasts of June precipitation were made by regressing rainfall data against two tidal frequencies at specific locations to quantify local responses to the forcing. These regressions showed larger explained variances than could reasonably have been expected by chance, thus strengthening the premise that tidal forces have nontrivial effects on the monsoon onset. Also, the success rate of these year-in-advance forecasts in northern India significantly exceeded that expected for random forecasts. Forecasts based on the tidal theory were correct much more often than persistence forecasts in this region. The statistical analyses of the rainfall variations and test predictions suggest that mechanical tidal forcing exists in the atmosphere and, when better understood, offers the potential of a useful long-range forecast tool.

Horizontal tidal forces are not limited to India, but in other areas of the world the number and complexity of meteorological factors enormously complicate quantification of atmospheric response. However, there is the good possibility that tidal effects may be nonnegligible, even in mid-latitudes. Research should be undertaken to determine how, where and when these may be observed and used for prediction. It seems likely that when other forces balance or where centers of action or high-gradient regions are involved, the effects of tidal forcing will be identifiable.

Acknowledgments. The authors are indebted to Pat Behling for skillfully managing the data base used in this study. Thanks also go to Brian Goodman for developing the program to calculate the soli-lunar tidal potential. The anonymous reviewers had constructive comments which greatly strengthened the statistical basis of this paper.

Much of the research support came from an anonymous donor to whom we are grateful. This project was also supported by the National Science Foundation (Grant ATM77-15213) and the National Oceanic and Atmospheric Administration (04-6-158-44071). In addition, Dr. J. B. Blechman was supported by a Postdoctoral Fellowship from the National Oceanic and Atmospheric Administration (Grant NA80AA-D-00117) for one year, part of which was spent in the course of this research. Major W. H. Campbell is at the University of Wisconsin-Madison under the Air Force Institute of Technology program.

REFERENCES

Adderley, E. E., and E. G. Bowen, 1962: Lunar component in precipitation data. *Science*, **137**, 749–750.

Bjerknes, J., 1969: Atmospheric teleconnections from the equatorial Pacific. *Mon. Wea. Rev.*, **97**, 163–172.

Brier, G. W., 1968: Long-range predictions of the zonal westerlies and some problems in data analysis. *Rev. Geophys.*, **6**, 525–551.

——, and D. A. Bradley, 1964: The lunar synodical period and precipitation in the United States. *J. Atmos. Sci.*, **21**, 386–395.

Bryson, R. A., 1948: On a lunar bi-fortnightly tide in the atmosphere. *Trans. Amer. Geophys. Union*, **29**, 473–475.

——, and T. B. Starr, 1977: Chandler tides in the atmosphere. *J. Atmos. Sci.*, **34**, 1975–1986.

——, and B. M. Goodman, 1980: Volcanic activity and climatic change. *Science*, **207**, 1041–1044.

Currie, R. C., 1981: Evidence for 18.6 year M_N signal in temperature and drought conditions in North America since AD 1800. *J. Geophys. Res.*, **86**, 11 055–11 064.

Das, P. K., 1968: *The Monsoon.* National Book Trust, New Delhi, 162 pp.

Doodson, A. T., 1921: The harmonic development of the tide generating potential. *Proc. Roy. Soc. London*, **A100**, 305–329.

Kidson, J. W., 1975: Eigenvector analysis of monthly mean surface data. *Mon. Wea. Rev.*, **103**, 177–186.

Lund, I. A., 1965: Indications of a lunar synodical period in United States observations of sunshine. *J. Atmos. Sci.*, **22**, 24–39.

Mills, C. A., 1966: Extraterrestrial factors in the initiation of North American polar fronts. *Mon. Wea. Rev.*, **94**, 313–318.

Overland, J. E., and R. W. Preisendorfer, 1982: A significance test for principal components applied to a cyclone climatology. *Mon. Wea. Rev.*, **110**, 1–4.

Picaut, J., and M. Verstraete, 1979: Propagation of a 14.7-day wave along the northern coast of the Guinea Gulf. *J. Phys. Oceanogr.*, **9**, 136–149.

Rao, Y. P., 1976: *Southwest Monsoon.* Indian Meteor. Dept., Poona, 367 pp.

Rasmusson, E. M., and T. H. Carpenter, 1982: Variations in tropical sea surface temperature and surface wind fields associated with the Southern Oscillation/El Niño. *Mon. Wea. Rev.*, **110**, 354–384.

Smart, W. M., 1971: *Spherical Astronomy.* Cambridge University Press, 430 pp.

Walker, G. T., 1924: Correlation in seasonal variations of weather, IX: A further study of world weather. *Mem. Indian Meteor. Dept.*, **24**, 275–332.

Walsh, J. E., and A. Mostek, 1980: A quantitative analysis of meteorological anomaly patterns over the United States, 1900–1977. *Mon. Wea. Rev.*, **108**, 615–630.

Wright, P. B., 1967: Changes in 200 mb circulation patterns related to the development of the Indian south-west monsoon. *Meteor. Mag.*, **96**, 302–315.

——, 1978: The Southern Oscillation. *Climatic Change and Variability*, A. B. Pittock, L. A. Frakes, D. Jenssen, J. A. Paterson and J. W. Zillman, Eds., Cambridge University Press, 180–185.

Yin, M. T., 1949: A synoptic-aerologic study of the onset of the summer monsoon over India and Burma. *J. Meteor.*, **6**, 393–400.